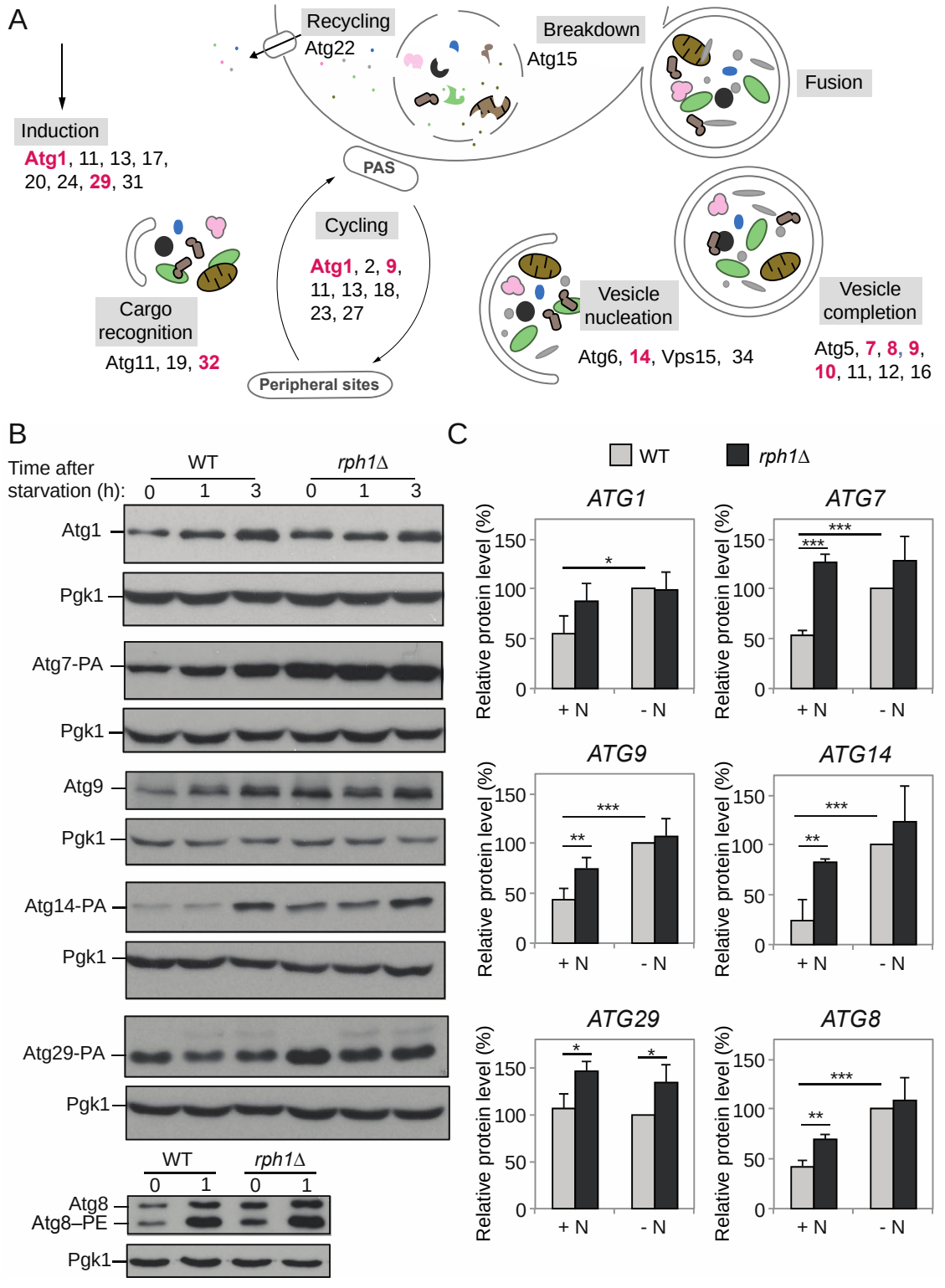

Figure S1, Related to Figure 1. Rph1 represses the expression of nitrogen-sensitive *ATG* genes in nutrient-replete conditions

(A) Schematic of the autophagy pathway; *ATG* genes analyzed in this study are highlighted in pink. PAS, phagophore assembly site.

(B) Rph1 represses the expression of the Atg1, Atg7, Atg8, Atg9, Atg14 and Atg29 proteins. Cells were grown in YPD until mid-log phase and then starved for nitrogen for the indicated times. For the analysis of Atg1, Atg8 and Atg9, wild-type (YTS158, BY4742) and *rph1*Δ (YAB300) cells were used; protein extracts were analyzed by western blot with antibodies to the indicated proteins. Pgk1 was used as a loading control. For the analysis of Atg7, Atg14 and Atg29 the corresponding genes were fused to the protein A coding sequence on the chromosome in either wild-type (YTS158, BY4742) or *rph1*Δ (YAB300) cells. Cells were collected and protein extracts were analyzed by western blot with either an antibody that detects PA or anti-Pgk1 (loading control) antiserum.

(C) Quantification of (B). The protein level of individual Atg proteins in rich conditions (+N) and after 3 h of starvation (-N) was normalized to the Pgk1 signal. Results present protein levels as percentage of the corresponding protein in wild-type cells after starvation, which was set to 100%. Error bars indicate the standard deviation of the average of at least 3 independent experiments.

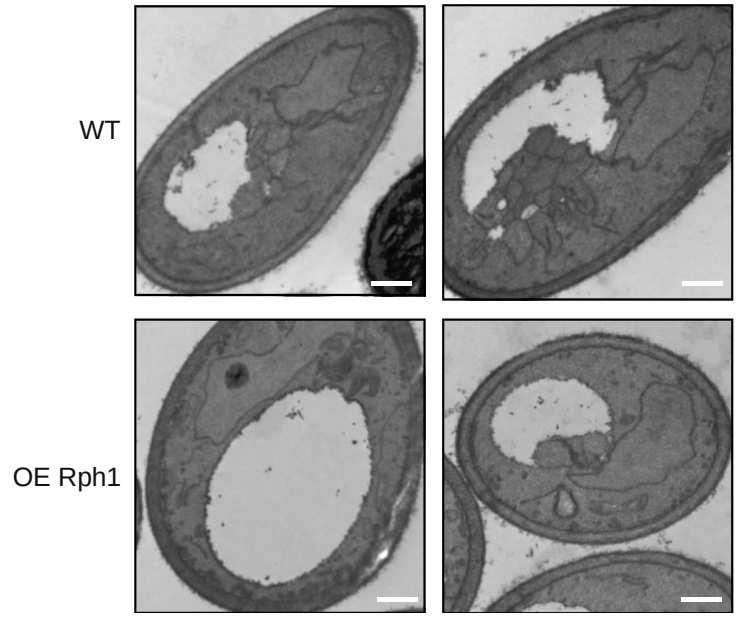

Figure S2, Related to Figure 4. The overexpression of Rph1 blocks the biogenesis of autophagic bodies

Wild-type cells (WT, FRY143) and cells overexpressing Rph1 (OE Rph1, YAB346) were imaged using transmission electron microscopy after 2h of nitrogen starvation. Representative TEM images showing a reduced accumulation of autophagic bodies in the vacuole of cells overexpressing Rph1 compared to wild type. Scale bar, 500 nm.

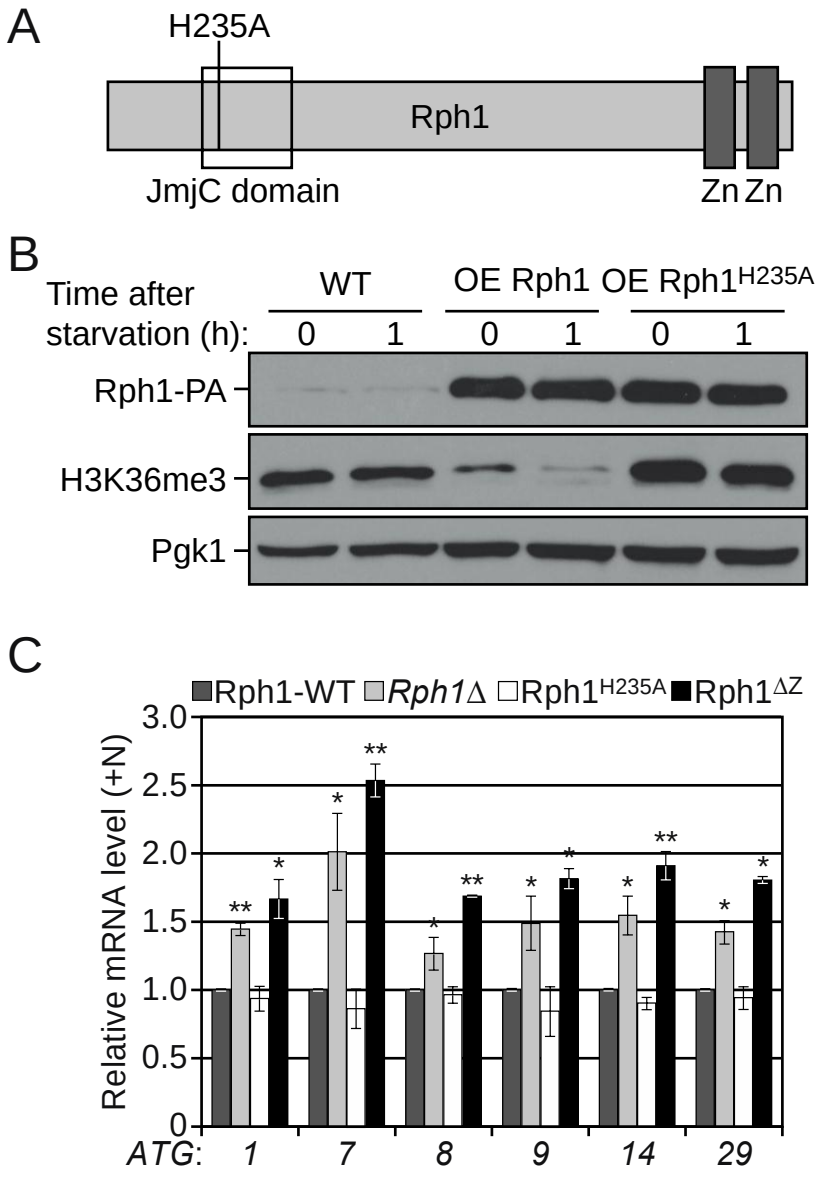

Figure S3, Related to Figure 5. Rph1 DNA binding ability but not histone demethylase activity is required for its function in autophagy

(A) Schematic of the Rph1 protein indicating the relative position of histidine H235 in the Jumonji C (JmjC) domain as well as the zinc-finger (Zn) DNA-binding domains.

(B) The mutation of H235 to an alanine inhibits Rph1 demethylase activity. In contrast to the overexpression of Rph1, which leads to a drastic reduction in tri-methylation at H3K36, overexpressing Rph1^{H235A} had no effect on H3K36me3. Rph1-PA cells (WT,

YAB366) and cells overexpressing Rph1-PA (OE Rph1, YAB363) or Rph1^{H235A}-PA (OE Rph1^{H235A}, YAB364) were grown in YPD until mid-log phase and then starved for nitrogen for 1 h. Cells were collected and protein extracts were analyzed by western blot with either an antibody that detects PA, H3K36me3 or anti-Pgk1 (loading control) antiserum.

(C) *rph1*Δ cells were transformed with the *RPH1p-RPH1-PA* (Rph1-WT), *RPH1p-RPH1^{H235A}-PA*, or *RPH1p-RPH1$^{\Delta Z}$-PA* plasmids or the corresponding empty plasmid (*pRS461-PA, rph1*Δ). Cells were grown in rich selective medium (SMD-ura) until mid-log phase and then starved for nitrogen for 1 h. Total RNA of cells in mid-log phase was extracted and the mRNA levels were quantified by RT-qPCR. Data represent the average of 3 independent experiments. Error bars indicate the standard deviation.

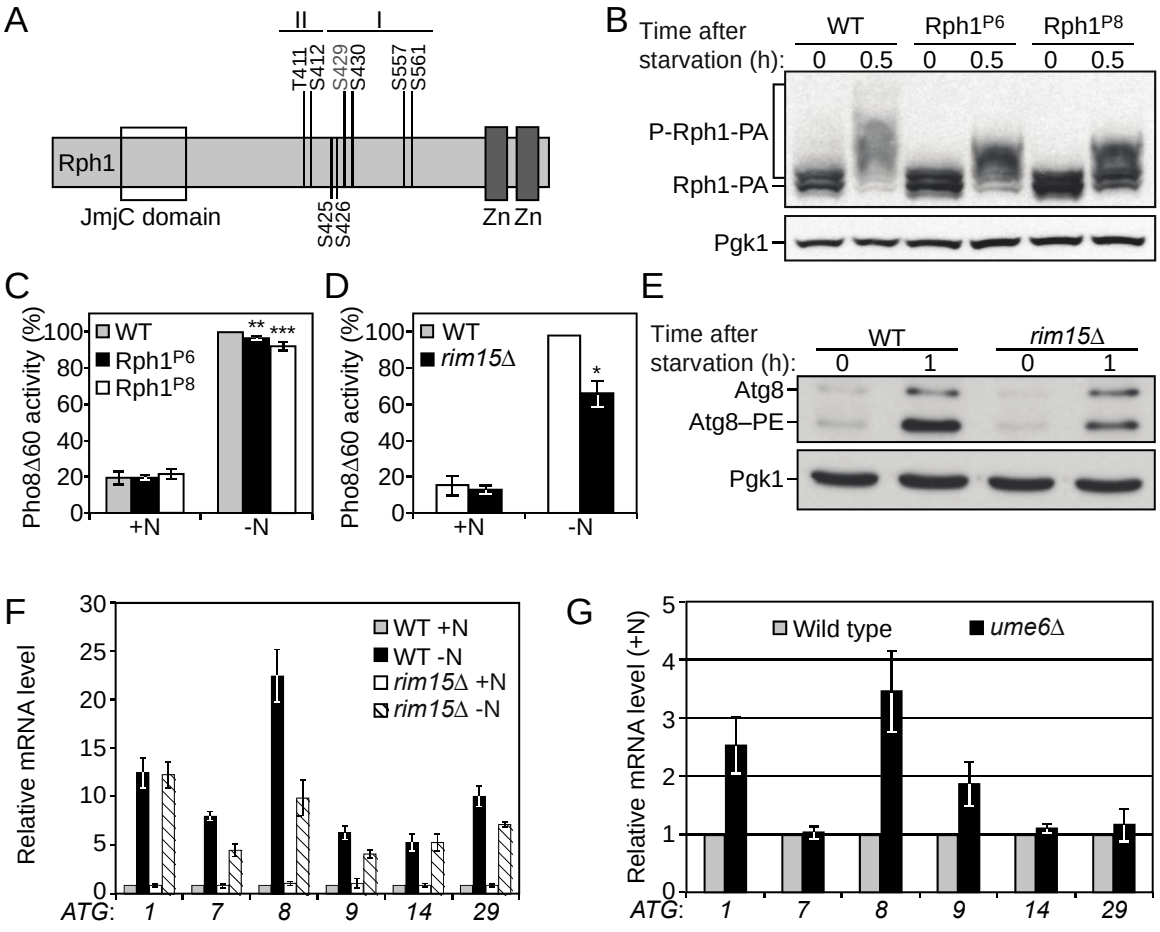

Figure S4, Related to Figure 6. Rim15-dependent phosphorylation of Rph1 upon nitrogen starvation releases its repression on *ATG* gene expression and autophagy

(A) Schematic of the Rph1 protein indicating the relative position of putative autophagy-dependent phosphorylated residues in Rph1. The Jumonji C (JmjC) domain as well as the zinc-finger (Zn) DNA-binding domains are indicated.

(B-C) The mutation of Rph1 putative phosphorylation sites partially inhibits Rph1 phosphorylation and autophagy upon nitrogen starvation. Wild-type (WT, YAB374, BY4742), Rph1^{P6} (YAB375, S425A-S426S-S429A-S430A-S557S-S561A) and Rph1^{P8} (YAB376, T411A-S412A-S425A-S426S-S429A-S430A-S557S-S561A) cells were grown until mid-log phase and then starved for the indicated time.

(B) Cells were collected and protein extracts were analyzed by western blot from gels containing 50 μM Phos-tag, with an antibody that detects PA or anti-Pgk1 (loading control) antiserum.

(C) Autophagy as measured by the Pho8Δ60 assay shows a minor decrease in Rph1 phosphomutants. Cells were starved for nitrogen (-N) for 2 h. The Pho8Δ60 activity was measured and normalized to the activity of wild-type cells after starvation, which was set to 100%. Error bars indicate the standard deviation of at least 3 independent experiments.

(D) Autophagy as measured by the Pho8Δ60 assay is decreased in *rim15*Δ cells. Wild-type (YAB308, BY4742) and *rim15*Δ (YAB341) cells were grown in YPD (+N) and then starved for nitrogen (-N) for 3 h. The Pho8Δ60 activity was measured and normalized to the activity of wild-type cells after starvation, which was set to 100%. Error bars indicate the standard deviation of 3 independent experiments.

(E) The deletion of *RIM15* causes a decrease in Atg8 protein level. WT (YAB308, BY4742) and *rim15*Δ cells (YAB341) were grown in YPD until mid-log phase and then starved for nitrogen for the indicated times. Cells were collected and protein extracts were analyzed by western blot with anti-Atg8 and anti-Pgk1 (loading control) antisera.

(F) The deletion of *RIM15* reduces the induction of *ATG* gene expression after nitrogen starvation. Wild type (WT; YAB308, BY4742) and *rim15*Δ (YAB341) cells were grown in YPD until mid-log phase (+N) and then starved for 1 h (-N). Total RNA was extracted and the mRNA levels were quantified by RT-qPCR. The mRNA level of individual *ATG* genes was normalized to the mRNA level of the corresponding gene in WT cells in rich conditions (+N), which was set to 1. Data represent the average of at least 3 independent experiments ± standard deviation.

(G) Ume6 represses the expression of *ATG1*, *ATG8* and *ATG9* but not *ATG7* and *ATG29* in growing-conditions. WT (BY4742) and *ume6*Δ cells were grown in YPD until mid-log phase (+N). Total RNA was extracted and the mRNA levels were quantified by RT-qPCR. The mRNA level of individual *ATG* genes was normalized to the mRNA level of the corresponding gene in WT cells, which was set to 1. Data represent the average of 3 independent experiments. Error bars indicate the standard deviation.

Table S1, Related to Figure 1. Strains used in this study

Name	Genotype	Reference
BY4742	*MATα his3Δ1 leu2Δ0 ura3Δ0*	ResGen/Invitrogen
FRY143	SEY6210, *pep4Δ::LEU2 vps4Δ::TRP1*	[S1]
SEY6210	*MATα his3Δ200 leu2-3,112 lys2-801 suc2-Δ9 trp1Δ901 ura3-52*	[S2]
ume6Δ	*BY4742 ume6Δ::KanMX6*	Invitrogen
WLY176	SEY6210 *pho13Δ pho8::pho8Δ60*	[S3]
WLY192	WLY176, *atg1Δ::HIS5*	[S4]
YAB288	WLY176, *rph1Δ::LEU2*	This study
YAB292	YTS158, *atg7Δ::HIS5*	This study
YAB300	YTS158, *rph1Δ*	This study
YAB301	YTS158, *gis1Δ*	This study
YAB302	YTS158, *rph1Δ gis1Δ*	This study
YAB312	YTS158, *Atg7-PA::HIS5*	This study
YAB313	YAB300, *Atg7-PA::HIS5*	This study
YAB314	YAB301, *Atg7-PA::HIS5*	This study
YAB315	YAB302, *Atg7-PA::HIS5*	This study
YAB318	YTS158, *set2Δ::HIS5*	This study
YAB308	YTS158, *Rph1-PA::HIS5*	This study
YAB323	WLY176, *Rph1-PA::HIS5*	This study
YAB329	YAB323, *ZEO1p-Rph1::KanMX6*	This study
YAB341	YAB308, *rim15Δ::URA3*	This study
YAB342	YAB312, *rim15Δ::URA3*	This study
YAB346	FRY143, *ZEO1p-Rph1::KanMX6*	This study
YAB347	YAB313, *rim15Δ::URA3*	This study
YAB348	YTS158, *Atg14-PA::His5*	This study
YAB349	YAB300, *Atg14-PA::His5*	This study
YAB350	YTS158, *Atg10-PA::HIS5*	This study
YAB351	YAB300, *Atg10-PA::HIS5*	This study
YAB352	YAB301, *Atg10-PA::HIS5*	This study
YAB353	YAB302, *Atg10-PA::HIS5*	This study
YAB354	YTS158, *Atg29-PA::His5*	This study
YAB355	YAB300, *Atg29-PA::His5*	This study
YAB363	YAB288, *ZEO1p-Rph1-PA::URA3*	This study
YAB364	YAB288, *ZEO1p-Rph1H235A-PA::URA3*	This study
YAB366	YAB288, *RPH1p-Rph1-PA::URA3*	This study
YAB374	YAB300, *RPH1p-Rph1-PA::URA3*	This study
YAB375	YAB300, *RPH1p-Rph1-S425A-S426A-S429A-S430A-S557A-S561A-PA::URA3*	This study
YAB376	YAB300, *RPH1p-Rph1-T411A-S412A-S425A-S426A-S429A-S430A-S557A-S561A-PA::URA3*	This study
YTS158	BY4742, *pho13Δ::KanMX6 pho8::pho8Δ60*	[S5]

Table S2, Related to Figure 1. RT-qPCR primers used in this study

Gene name	Sequence (5' 3')
ATG1 F	ATCTAAGATGGCCGCACATATG
ATG1 R	AGGGTAGTCACCATAGGCATTC
ATG7 F	ATGAGCATTGTCCAGCATGTAG
ATG7 R	GACCTCCTGCTTTATGACTGAC
ATG8 F	GAAGGCCATCTTCATTTTTGTC
ATG8 R	TTCTCCTGAGTAAGTGACATAC
ATG9 F	CGTACTAACAGAGTCTTTCCTTG
ATG9 R	CTAAGACACCACCCTTATTGAG
ATG14 F	TACTGGACCAGTACGATGTG
ATG14 R	TGCAGGATGTCCTCTTTGTG
ATG29 F	ATGAGGCGTTACAACATTTGC
ATG29 R	TCGTCATCTGAACTACCGCAC
TAF10 F	ATATTCCAGGATCAGGTCTTCCGTAGC
TAR10 R	GTAGTCTTCTCATTCTGTTGATGTTGTTGTTG
TFC1 F	GCTGGCACTCATATCTTATCGTTTCACAATGG
TFC1 R	GAACCTGCTGTCAATACCGCCTGGAG
WIPI1 F	TCCAGTGGACACCTTTATATG
WIPI1 R	AGCTGTGGGTTTTGATTAAG
mATG7 F	GATTGTCCTAAAGCAGTTGG
mATG7 R	CTTTTAGGGTCCATACATTCAC
mATG14 F	AATTTACTCGAGCAGTGAAG
mATG14 R	TTAGATTCCTGAGGGTATGC
MAP1LC3B F	ATAGAACGATACAAGGGTGAG
MAP1LC3B R	CTGTAAGCGCCTTCTAATTATC
GAPDH F	ACAGTTGCCATGTAGACC
GAPDH R	TTTTTGGTTGAGCACAGG
ACTB F	GATCAAGATCATTGCTCCTC
ACTB R	TTGTCAAGAAAGGGTGTAAC
ATG7 ChIP F	TGGAAGAACAAGCCACCACATG
ATG7 ChIP R	GGGTGTCCAAAGGAATCTCATG
PHR1 ChIP F	GGGTGAAAGTATGCTTACTTTGAC
PHR1 ChIP R	ACAATCTCCATTGGTTTAGCCC
ChrVI ChIP F	ATTCCAAACGGTGTTCCTTTAC
ChrVI ChIP R	AAAGTAAACGGTGGTCTCTGTG

Table S3, Related to Figure 4. WT vs. OE Rph1 TEM data

	Autophagic body size					**Vacuole size**				**Autophagic body number**	
	Measured cross-sectional		Estimated original			Measured cross-sectional		Estimated original		Measured cross-sections/cell	Estimated bodies/cell
	Mean rad (nm)	SD rad (nm)	Mean rad (nm)	SD rad (nm)	Volume (nm^3)	Mean rad (nm)	SD rad (nm)	Mean rad (nm)	SD rad (nm)		
WT	157.5	55.3	175.5	48.5	2.82E+07	840.5	232.7	923.3	212.1	5.53	23.13
OE Rph1	145.9	46.5	164.3	38.5	2.18E+07	835.6	236	912.2	216.8	1.72	1.72

Table S4, Related to Figure 5. Analysis of Rph1 binding motifs in *ATG* promoters

	Rph1 DNA binding motifs								
Gene name	2162	279	547	1087	2228	1088	1699	1252	TWAGGG
ATG1									
ATG2				1				1	
ATG3									
ATG4									
ATG5						2			
ATG6									
ATG7	**1**			**2**					**1**
ATG8	**1**	**2**							
ATG9	**1**	**1**	**1**	**1**		**1**			**1**
ATG10								1	
ATG11									
ATG12					1	1			
ATG13						1			
ATG14	**1**								**1**
ATG15						1			
ATG16				1		1			
ATG17	1								1
ATG18									
ATG19	1	1				1		1	
ATG20	1	1		1		2			1
ATG21				1		1			
ATG22				1	1				
ATG23									
ATG24		1		1					
ATG26								1	
ATG27									
ATG29	**1**	**1**				**1**			
ATG31									
ATG32				**1**					
ATG33	1								1
ATG34	1	1	1			1		1	1
ATG36						1			
Total occurrence in *ATG* promoters									
	10	8	2	10	2	14	0	5	7
	5	**4**	**1**	**4**	**0**	**2**	**0**	**0**	**3**

Promoter regions of *ATG* genes were analyzed using the online software YetFasCo (available at http://yetfasco.ccbr.utoronto.ca). The number of occurrence of each motif is indicated. Genes upregulated in the *RPH1* deletion strain (Figure 1A) are highlighted. See Table S5 for motif identities.

Table S5, Relative to Figure 5. Rph1 DNA binding motifs

Rph1 DNA binding motifs #		References
2162		[S6]
823		[S7]
279	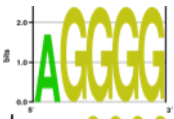	[S8]
547	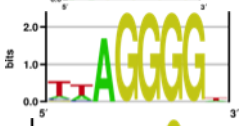	[S9]
1085	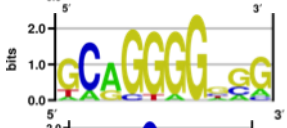	[S10]
1087	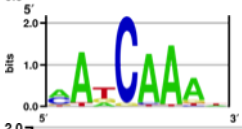	[S10]
2228		[S11]
675		[S11]
1862	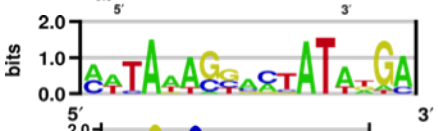	[S12]
1698	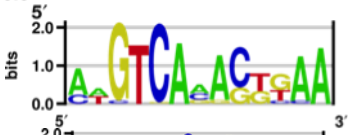	[S12]
1697		[S12]
1088		[S10]
1086		[S10]
1699		[S12]
1252		[S13]

Supplemental Experimental Procedures

Plasmids

The *pRS416-PA* plasmid was constructed by inserting two copies of the protein A open reading frame (ORF) followed by the *ADH1* terminator in the pRS416 plasmid between the XbaI and EcoRI sites. For constructing the plasmid *ATG7p-ATG7-PA*, (where "*ATG7p*" indicates the promoter of the *ATG7* gene), the *ATG7* ORF and promoter region (-800-0) was amplified by PCR, digested by SacII and NotI and ligated into the *pRS416-PA* plasmid. For constructing the plasmids *GAL3p-ATG7-PA*, *FLO5p-ATG7-PA* and *SEF1p-ATG7-PA*, a region of approximately 800 bp upstream of the corresponding ORF was amplified by PCR and fused to a PCR-amplified *ATG7* ORF by overlapping PCR. The resulting products were digested by SacII and NotI and ligated into the *pRS416-PA* plasmid. The *RPH1p-RPH1-PA* plasmid was constructed by amplifying the *RPH1* ORF and promoter region (-500-0) by PCR followed by digestion with NotI and XbaI and ligation into the *pRS416-PA* plasmid. The *RPH1p-RPH1*^{H235A}*-PA* plasmid was constructed by amplifying (1) the *RPH1* ORF and promoter region up to the sequence corresponding to histidine 235 with a reverse primer containing the histidine-to-alanine mutation and (2) the *RPH1* ORF starting from the sequence corresponding to histidine 235 until the last codon before the stop codon with a forward primer containing the histidine to alanine mutation. *RPH1p-RPH1*^{H235A} was amplified by overlapping PCR using the PCR (1) and PCR (2) products resulting from the previous step as template, digested by NotI and XbaI and ligated into *pRS416-PA*. The *RPH1p-RPH1*$^{\Delta Z}$*-PA* plasmid was constructed by amplifying (1) the *RPH1* ORF and promoter region up to the sequence corresponding to the first zinc-finger domain with a reverse primer containing

the inter zinc-domain sequence and (2) the *RPH1* ORF starting from the sequence following the last zinc-finger domain until the last codon before the stop codon with a forward primer containing the inter zinc-domain sequence. *RPH1p-RPH1*$^{\Delta Z}$ was amplified by overlapping PCR using the PCR (1) and PCR (2) products resulting from the previous step as template, digested by NotI and XbaI and ligated into *pRS416-PA*. For constructing the strains YAB363, YAB364 and YAB366, *RPH1p-RPH1-PA*, *ZEO1p-RPH1-PA* and *ZEO1p-RPH1*^{H235A}*-PA* were generated as described above, digested by NotI and SalI and ligated into *pRS406*. The resulting plasmids were digested by NcoI (for integration at the *URA*3 locus). For generating the strains YAB374, YAB375 and YAB376, we constructing the following plasmids: *RPH1p-RPH1-PA(406), RPH1p-Rph1-S425A-S426A-S429A-S430A-S557A-S561A-PA(406)* and *RPH1p-Rph1-T411A-S412A-S425A-S426A-S429A-S430A-S557A-S561A-PA(406)*. The *RPH1* ORF and promoter region was amplified as previously described. Mutations were introduced by overlapping PCR as described above. Inserts were digested by NotI and SalI and ligated into *pRS406*. The resulting plasmids were digested by AflII (for integration at the *RPH1* promoter).

RNA and RT-qPCR

To eliminate genomic DNA contamination after total RNA extraction, an additional DNase treatment was performed according to the RNeasy kit instruction with the RNase-free DNase set (Qiagen). One microgram of total RNA was reverse-transcribed into cDNA in a 20-µl reaction mixture. The cDNA levels were then analyzed using the Eppendorf Realplex^4 with the gene-specific primers listed in Table S2. Each sample was

tested in a 96-well plate (Applied Biosystems). The reaction mix (15-µl final volume) consisted of 7.5 µl of Power SYBR Green master mix (Applied Biosystems), 0.5 µl of each primer (333.3 nM final concentration), 1.5 µl of H_2O, and 5 µl of a 1/5 dilution of the cDNA preparation. The thermocycling program consisted of one hold at 95°C for 10 min, followed by 40 cycles of 15 s at 95°C and 1 min at 60°C. After completion of these cycles, melting-curve data were then collected to verify PCR specificity and the absence of primer dimers, and to examine potential contamination. The transcript abundance in samples was determined using a comparative threshold cycle method. The relative abundance of the reference mRNAs of *TAF10* and *TFC1* [S14] in each sample was determined and used to normalize for differences of total RNA amount according to the method described by Vandesompele et al. [S15]. Unless specified, the mRNA level of individual *ATG* genes was normalized to the mRNA level of the corresponding gene in wild-type cells grown in rich conditions, which was set to 1.

Chromatin Immunoprecipitation

Minor modifications to the ChIP procedure were as follows: Rph1-PA and Rph1$^{\Delta Z}$-PA were affinity isolated with Dynabeads® (Life technologies) coupled to purified human IgG (Invitrogen) according to the Dynabeads® Antibody Coupling Kit directions (Life technologies). Primers used for ChIP are listed in Table S2.

Lambda Protein Phosphatase Treatment

The equivalent of 5 OD units of yeast cells were lysed in 50 µl of λ-phosphatase buffer (New England Biolabs) supplemented with 1% Triton X-100, 0.1% sodium

deoxycholate, 1 mM PMSF, protease inhibitor cocktail (ProBlock^{TM}-50, Gold Biotechnology), with or without phosphatase inhibitor cocktail (PhosSTOP, Roche). A 2.5-µl aliquot of lysate was used as template in a 50-µl reaction with λ-phosphatase buffer, 1 mM $MnCl_2$ and with or without 1200 units of λ-phosphatase (New England Biolabs). The samples were incubated at 30°C for 1.5 h. The reaction was stopped and proteins were precipitated by addition of 10% trichloroacetic acid.

Other Methods

Protein extraction, immunoblot, GFP-Atg8 processing, and alkaline phosphatase (Pho8Δ60) assays were performed as previously described [S16-S17, 28]. Phos-tag was used according to the manufacturer's (Wako) instruction at a final concentration of 50 µM. Antisera to Atg8 [S18], Atg1 [S19], Atg9 [S20], Pgk1 (a generous gift from Dr. Jeremy Thorner, University of California, Berkeley), monoclonal YFP (JL-8, Clontech) a commercial antibody that reacts with PA (anti-PA, no longer available), and anti-H3K36m3 (Active Motif, 61101) were used as previously described.

Mammalian Cell Transfection

Transfection was performed in 6-well dishes using a final siRNA concentration of 50 nM and 7 µl of transfection reagent. The medium was changed 3 h after transfection. *KDM4A* (L-004292) and non-targeting ON-TARGET (D-001810) SMARTpool siRNAs were purchased from Dharmacon. HeLa cells were transfected with a *KDM4A* plasmid or pcDNA using 6 µl Xtreme Gene HP Reagent (Roche)/2 µg of DNA per well in a 6-well

dish. The medium was changed 3 h after transfection. The *KDM4A* overexpression plasmid was a generous gift from Dr. Kristian Helin (University of Copenhagen, BRIC).

Tandem Fluorescence Reporter Flux Assay

The green fluorescence of the tandem reporter mRFP-GFP-LC3 is attenuated in the acidic pH lysosomal environment, whereas the mRFP is not. Therefore, the green fluorescent component of the composite yellow fluorescence (green + red = autophagosome) from the mRFP-GFP-LC3 reporter is lost upon autophagosome fusion with a lysosome, whereas the red fluorescence (red = autolysosome) remains detectable. At 24 h after plating, the cells were transfected with the mRFP–GFP–LC3 plasmid using 6 µl Xtreme Gene HP Reagent (Roche)/2 µg of DNA per well in a 6-well dish. The medium was changed 3 h after transfection. On the subsequent day cells were transfected with siRNA as described above. The next day, cells were treated for an extra 24 h with the indicated compounds (DMSO or 250 nM Torin1). Cells were then fixed using 4% paraformaldehyde, nuclei were stained with Hoechst, and autophagy was determined by quantification of the number of cells with LC3-positive puncta; cells with at least 5 detectable LC3 puncta were considered positive. The mRFP-GFP-LC3 plasmid was a kind gift of Dr. Tamotsu Yoshimori (National Institute of Genetics, Mishima, Japan).

Mammalian Cell Western Blot

Cells were seeded in 6-well dishes and on the subsequent day transfected using Xtreme Lipofectamine 2000 (see above). After 3 h of transfection the medium was changed and on the next day the indicated wells were treated with bafilomycin A_1 (40 nM). Total cell

lysate was harvested 48 h after transfection using Laemmli buffer and a cell scraper. Extracts were sonicated and subsequently boiled for 6 min at 96°C. SDS-PAGE was run using 15% acrylamide gels. Proteins were subsequently transferred to nitrocellulose (0.2-µm pores) using wet transfer (Bio-Rad). Primary antibodies were purchased from Sigma (KDM4A, HPA007610; actin A3853; MAP1LC3B, L7543) or USBiological Life Sciences (JMJD2A phosphorylated at Y547, 037196).

Mammalian RNA qPCR

For analysis of RNA expression, HeLa cells were seeded in a 6-well dish. At 24 h after plating, the cells were transfected with siRNA (see above). The medium on the cells was changed after 3 h transfection and cells were grown for another 45 h (48 h total after transfection). RNA was extracted using the RNeasy Kit (Qiagen) performing on-column DNAse digestion. RNA concentration was determined using Nanodrop, and 1µg of total RNA was used for first strand synthesis with SuperScript II Reverse Tanscriptase (Invitrogen). QPCR was run on an ABI 7500 and *GAPDH* or *ACTB* was used as a housekeeping gene for normalization. All primers were predesigned oligos (used at 4 nM/well) purchased from Sigma (KiCqStart). qPCR analysis and statistical analysis was done using R.

Statistical analyses

Statistical differences were assayed using one-sample *t* test and student *t* test; *$p<0.05$, **$p<0.01$, ***$p<0.001$.

Supplemental References

S1. Cheong, H., Yorimitsu, T., Reggiori, F., Legakis, J.E., Wang, C.-W., and Klionsky, D.J. (2005). Atg17 regulates the magnitude of the autophagic response. Mol Biol Cell *16*, 3438-3453.

S2. Robinson, J. S., Klionsky, D. J., Banta, L. M., and Emr, S. D. (1988). Protein sorting in *Saccharomyces cerevisiae*: isolation of mutants defective in the delivery and processing of multiple vacuolar hydrolases. Mol Cell Biol *8*, 4936-4948.

S3. Mao, K., Chew, L.H., Inoue-Aono, Y., Cheong, H., Nair, U., Popelka, H., Yip, C.K., and Klionsky, D.J. (2013). Atg29 phosphorylation regulates coordination of the Atg17-Atg31-Atg29 complex with the Atg11 scaffold during autophagy initiation. Proc Natl Acad Sci U S A *110*, E2875-2884.

S4. Kanki, T., Wang, K., Baba, M., Bartholomew, C.R., Lynch-Day, M.A., Du, Z., Geng, J., Mao, K., Yang, Z., Yen, W.-L., and Klionsky, D.J. (2009). A genomic screen for yeast mutants defective in selective mitochondria autophagy. Mol Biol Cell *20*, 4730-4738.

S5. He, C., Song, H., Yorimitsu, T., Monastyrska, I., Yen, W.-L., Legakis, J. E., and Klionsky, D. J. (2006). Recruitment of Atg9 to the preautophagosomal structure by Atg11 is essential for selective autophagy in budding yeast. J Cell Biol *175*, 925-935.

S6. Zhao, Y., Granas, D., and Stormo, G.D. (2009). Inferring binding energies from selected binding sites. PLoS Comput Biol *5*,e1000590.

S7. Zhu, C., Byers, K.J., McCord, R.P., Shi, Z., Berger, M.F., Newburger, D.E., Saulrieta, K., Smith, Z., Shah, M.V., Radhakrishnan, M., Philippakis, A.A., Hu, Y., De Masi, F., Pacek, M., Rolfs, A., Murthy, T., Labaer, J., and Bulyk, M.L. (2009). High-resolution DNA-binding specificity analysis of yeast transcription factors. Genome Res *19*, 556-566.

S8. Jang, Y.K., Wang, L., and Sancar, G.B. (1999). *RPH1* and *GIS1* are damage-responsive repressors of *PHR1*. Mol Cell Biol *19*, 7630-7638.

S9. Badis, G., Chan, E.T., van Bakel, H., Pena-Castillo, L., Tillo, D., Tsui, K., Carlson, C.D., Gossett, A.J., Hasinoff, M.J., Warren, C.L., Gebbia, M., Talukder, S., Yang, A., Mnaimneh, S., Terterov, D., Coburn, D., Li Yeo, A., Yeo, Z.X., Clarke, N.D., Lieb, J.D., Ansari, A.Z., Nislow, C., and Hughes, T.R. (2008). A library of yeast transcription factor motifs reveals a widespread function for Rsc3 in targeting nucleosome exclusion at promoters. Mol Cell *32*, 878-887.

S10. Reddy, T.E., DeLisi, C., and Shakhnovich, B.E. (2007). Binding site graphs: a new graph theoretical framework for prediction of transcription factor binding sites. PLoS Comput Biol *3*, e90.

S11. MacIsaac, K.D., Wang, T., Gordon, D.B., Gifford, D.K., Stormo, G.D., and Fraenkel, E. (2006). An improved map of conserved regulatory sites for *Saccharomyces cerevisiae*. BMC Bioinformatics *7,* 7:113.

S12. Foat, B.C., Tepper, R.G., and Bussemaker, H.J. (2008). TransfactomeDB: a resource for exploring the nucleotide sequence specificity and condition-specific regulatory activity of trans-acting factors. Nucl Acids Res *36*, D125-31.

S13. Lee, T.I., Rinaldi, N.J., Robert, F., Odom, D.T., Bar-Joseph, Z., Gerber, G.K., Hannett, N.M., Harbison, C.T., Thompson, C.M., Simon, I., Zeitlinger, J., Jennings, E.G., Murray, H.L., Gordon, D.B., Ren, B., Wyrick, J.J., Tagne, J.-B., Volkert, T.L., Fraenkel, E., Gifford, D.K. and Young, R.A. (2002). Transcriptional regulatory networks in *Saccharomyces cerevisiae*. Science *298*, 799-804.

S14. Teste, M.A., Duquenne, M., François, J.M., and Parrou, J.L. (2009). Validation of reference genes for quantitative expression analysis by real-time RT-PCR in Saccharomyces cerevisiae. BMC Mol Biol *10*, 99.

S15. Vandesompele, J., De Preter, K., Pattyn, F., Poppe, B., Van Roy, N., De Paepe, A., and Speleman, F. (2002). Accurate normalization of real-time quantitative RT-PCR data by geometric averaging of multiple internal control genes. Genome Biol *3*, H0034.

S16. Yorimitsu, T., Zaman, S., Broach, J.R., and Klionsky, D.J. (2007). Protein kinase A and Sch9 cooperatively regulate induction of autophagy in *Saccharomyces cerevisiae*. Mol Biol Cell *18*, 4180–4189.

S17. Noda, T., Matsuura, A., Wada, Y., and Ohsumi, Y. (1995). Novel system for monitoring autophagy in the yeast *Saccharomyces cerevisiae*. Biochem Biophys Res Commun *210*, 126–132.

S18. Huang, W.-P., Scott, S.V., Kim, J., and Klionsky, D.J. (2000). The itinerary of a vesicle component, Aut7p/Cvt5p, terminates in the yeast vacuole via the autophagy/Cvt pathways. J Biol Chem *275*, 5845-5851.

S19. Abeliovich, H., Zhang, C., Dunn Jr., W.A., Shokat, K.M., and Klionsky, D.J. (2003). Chemical genetic analysis of Apg1 reveals a non-kinase role in the induction of autophagy Mol. Biol. Cell *14*,477–490.

S20. Noda, T., Kim, J., Huang, W.-P., Baba, M., , Tokunaga, C., Ohsumi, Y., and Klionsky, D.J. (2000). Apg9p/Cvt7p is an integral membrane protein required for transport vesicle formation in the Cvt and autophagy pathways J Cell Biol *148*, 465–480.